States of a two-dimensional photonic crystal in the presence of spatial modulation and anisotropy: A perturbative approach

G. Alagappan,[1,2] X. W. Sun,[1,3,*] and M. B. Yu[3]
[1]*School of Electrical and Electronic Engineering, Nanyang Technological University, Nanyang Avenue, Singapore 639798*
[2]*Institute of High Performance Computing, 1 Science Park Road, Science Park II, Singapore 117528*
[3]*Institute of Microelectronics, 11 Science Park Road, Science Park II, Singapore 117685*
(Received 6 February 2008; revised manuscript received 22 April 2008; published 11 July 2008)

This paper presents an analytic study on the photonic states of a two-dimensional photonic crystal. Degenerate states in the absence of spatial modulation are systematically classified and the states within the same class behave similarly when the spatial modulation or the material's anisotropy is switched on. In addition, employing reduced plane-wave basis, we illustrate a simple yet powerful approach to analytically approximate the splitting of the degenerate states in the presence of the spatial modulation and the material's anisotropy. Using hexagonal lattice photonic crystal as an example, we illustrate the accuracy and the applications of the approach.

DOI: 10.1103/PhysRevB.78.035112 PACS number(s): 42.70.Qs, 42.70.Df

I. INTRODUCTION

There are various existing methods such as plane-wave expansion method (PWM),[1–3] finite difference time domain,[4,5] transfer-matrix method,[6,7] and scattering matrix method[8–10] available for modeling of photonic crystals (PCs). Among these methods, PWM is the most widely used method in handling PC problems.[11] PWM has been used in computations of photonic band gaps,[1–3] equal frequency surfaces for the theory of light refraction[12–14] and diffraction,[15,16] Bragg transmittance and reflectance,[17,18] and spontaneous emission in a PC.[19,20] In the photonic band-structure calculation, the conventional PWM (Refs. 2 and 3) is also quite often modified (or extended) to handle specific PC structures or to increase the rate of convergence.[11,21–24] This includes the use of supercell techniques in modeling defects in PC,[21,22] the extension to include the effect of the interface,[23] augmented PWM for PCs with spherical and cylindrical motifs,[24] and the use of fast factorization rules in PWM.[11]

Unfortunately, none of these modifications in PWM or those of other methods is simple, as they all involve numerical methods without any analytical details or formulalike description. For example, the solution in PWM is found by diagonalizing a very large matrix with the size determined by the number of plane waves. The typical number of plane waves used in PWM calculations for PCs with large modulation ranges from $\sim 10^2$ to $\sim 10^3$.[2,3,12,25] For structures with small (but finite) spatial modulation, though they consume a slightly smaller number of plane waves, the approach still fails to provide any useful analytical details. In this paper, we present a systematic and generalized solution with analytical details based on PWM for two-dimensional (2D) PCs. In order to illustrate the approach, without losing generality, a hexagonal lattice 2D PC is used in this paper. We first analyze the photonic states in the limit of zero modulation (i.e., free photon relationship) for a 2D PC with isotropic materials and we have introduced a systematic classification system based on integers for the states with distinct frequencies. These integers can be factored and states with the same factor can be categorized as they have the same form of solution when the spatial modulation or/and the material's anisotropy is switched on. As we shall show, such states can be easily solved with a reduced matrix size and typically lead to analytical equations within a small (however a finite) spatial modulation approximation.

The presented method is useful in the applications which exploit the unusual conducting behavior of a PC, where conductions such as superprisms, supercolimation, beam splitting, etc. are only well pronounced in PCs will small spatial modulation.[26–29] Further in such PC structures, the method can be applied to obtain a fairly accurate solution for the insulating properties (i.e., band gaps). In a large refractive index contrast PC, the presented method likely leads to a deviated result, but the method surely serves a good approximation and produces necessary analytical details such as degeneracy of the state and the properties of a free photon behavior at the band edges.

II. EIGEN-EQUATIONS

Maxwell equations for periodic structures can be reduced to a time-independent eigen-equation,[1,11,30,31]

$$\nabla \times \frac{1}{\tilde{\varepsilon}(\mathbf{r})} \nabla \times \mathbf{H}_{\mathbf{k}}(\mathbf{r}) = \Omega(\mathbf{k}) \mathbf{H}_{\mathbf{k}}(\mathbf{r}), \tag{1}$$

where $\Omega(\mathbf{k})$ is the eigenvalue, $\tilde{\varepsilon}(\mathbf{r})$ is the position-dependent dielectric tensor,[30–32]

$$\tilde{\varepsilon}(\mathbf{r}) = \begin{pmatrix} \varepsilon_{11}(\mathbf{r}) & \varepsilon_{12}(\mathbf{r}) & \varepsilon_{13}(\mathbf{r}) \\ \varepsilon_{21}(\mathbf{r}) & \varepsilon_{22}(\mathbf{r}) & \varepsilon_{23}(\mathbf{r}) \\ \varepsilon_{31}(\mathbf{r}) & \varepsilon_{32}(\mathbf{r}) & \varepsilon_{33}(\mathbf{r}) \end{pmatrix}, \tag{2}$$

and $\mathbf{H}_{\mathbf{k}}(\mathbf{r})$ is the magnetic field in the Bloch form with a wave vector $\mathbf{k}$. Equation (1) is a set of coupled differential equations and decoupling of the equations depends on the dimension of the PC and the material's anisotropy. In a 2D PC with isotropic material, Eq. (1) can be decoupled into two independent equations corresponding to the two independent

TABLE I. The expressions $c_{\mathbf{k}}$, $m_{\mathbf{k}}$, $\alpha_{\mathbf{k}}$, and $p_{\mathbf{k}}$ for symmetrical $\mathbf{k}$-points of a hexagonal lattice. Key: $m=n_1^2+n_2^2-n_1n_2$.

				$p_{\mathbf{k}}$	
$\mathbf{k}$	$c_{\mathbf{k}}$	$m_{\mathbf{k}}$	$\sin(\alpha_{\mathbf{k}})$	$p_{\mathbf{k}}(n_1)$	$p_{\mathbf{k}}(n_2)$
Γ	4/3	m	$(2n_2-n_1)/\sqrt{3c_\Gamma m_\Gamma}$	$(3/4)n_1^2$	$(3/4)n_2^2$
K	4/9	$3(m+n_1)+1$	$(2n_2-n_1)/\sqrt{3c_K m_K}$	$(1/4)(2+3n_1)^2$	$(1/4)(1+3n_2)^2$
M	1/3	$2(2m+2n_2-n_1)+1$	$(2n_2-n_1+1)/\sqrt{3c_M m_M}$	$3n_1^2$	$(3/4)(1+2n_2)^2$

polarizations of light. If the material is anisotropic, then decoupling of the polarization requires one of the principal axes of the anisotropic material to be perpendicular to the 2D periodic plane.[31,32] As such, $\varepsilon_{13}(\mathbf{r})=\varepsilon_{31}(\mathbf{r})=\varepsilon_{23}(\mathbf{r})=\varepsilon_{32}(\mathbf{r})=0$, and consequently the Fourier coefficient matrix of the inverse of $\tilde{\varepsilon}(\mathbf{r})$ is

$$\tilde{\kappa}(\mathbf{G})=\begin{pmatrix}\kappa_{11}(\mathbf{G}) & \kappa_{12}(\mathbf{G}) & 0\\ \kappa_{21}(\mathbf{G}) & \kappa_{22}(\mathbf{G}) & 0\\ 0 & 0 & \kappa_{33}(\mathbf{G})\end{pmatrix}. \tag{3}$$

Using Eq. (3) and further expanding the fields in the plane-wave bases, Eq. (1) can be written in a normalized form as[30–32]

$$\sum_j M_{ij}H_j=\omega^2 H_i, \tag{4}$$

where $M_{ij}=|\mathbf{k}+\mathbf{G}_i||\mathbf{k}+\mathbf{G}_j|[\mathbf{e}_i\cdot\tilde{\kappa}_H(\mathbf{G}_i-\mathbf{G}_j)\cdot\mathbf{e}_j]$ and $M_{ij}=\kappa_E(\mathbf{G}_i-\mathbf{G}_j)|\mathbf{k}+\mathbf{G}_i||\mathbf{k}+\mathbf{G}_j|$ for H (magnetic field perpendicular to the periodic plane) and E (electric field perpendicular to the periodic plane) polarization, respectively. In these equations, H_i denotes a component of magnetic field, $\mathbf{G}_i$ is a reciprocal lattice vector, $\mathbf{e}_i$ is the unit vector perpendicular to both $\mathbf{k}+\mathbf{G}_i$ and electric field of E polarization, $\kappa_E(\mathbf{G})=\kappa_{33}(\mathbf{G})$ and $\tilde{\kappa}_H(\mathbf{G})$ takes the definition[32]

$$\tilde{\kappa}_H(\mathbf{G})=\begin{pmatrix}\kappa_{11}(\mathbf{G}) & \kappa_{12}(\mathbf{G})\\ \kappa_{21}(\mathbf{G}) & \kappa_{22}(\mathbf{G})\end{pmatrix}. \tag{5}$$

If all the materials are isotropic, we have $\kappa_{11}(\mathbf{G})=\kappa_{22}(\mathbf{G})=\kappa_{33}(\mathbf{G})=\kappa(\mathbf{G})$ and $\kappa_{12}(\mathbf{G})=\kappa_{21}(\mathbf{G})=0$. In Eq. (4), ω is the normalized frequency (i.e., ratio between period of the PC, a, and the free space wavelength) and both $\mathbf{k}$ and $\mathbf{G}$ have a unit of $2\pi/a$. The reciprocal lattice vector, $\mathbf{G}$, of any two-dimensional lattice can be written in terms of unit vectors $\mathbf{b}_1$ and $\mathbf{b}_2$ as $\mathbf{G}=n_1\mathbf{b}_1+n_2\mathbf{b}_2$, with n_1 and n_2 being any integers. The angle between $\mathbf{k}+\mathbf{G}$ vector and k_x axis of the reciprocal space is denoted as $\alpha_{\mathbf{k}}$, whereas the angle between $\mathbf{b}_1(\mathbf{b}_2)$ vector with k_x axis is denoted as $\alpha_{b1}(\alpha_{b2})$. For the hexagonal lattice, $\mathbf{b}_1=(1,-1/\sqrt{3})$, $\mathbf{b}_2=(0,2/\sqrt{3})$, $\alpha_{b1}=-30°$ and $\alpha_{b2}=90°$.

III. ABSENCE OF SPATIAL MODULATION

In the absence of a spatial modulation (i.e., a vanishingly small refractive index modulation), the photonic band structure must reduce to a free photon dispersion with the band folding effect taken into account.[1,12] In this case, only the Fourier coefficient, $\tilde{\kappa}(0)$ [Eq. (3)] is nonzero. Therefore, Eq. (4) reduces to

$$\omega^2=(\mathbf{k}+\mathbf{G})\cdot\tilde{\kappa}_H(0)\cdot(\mathbf{k}+\mathbf{G}) \tag{6a}$$

and

$$\omega^2=\kappa_{33}(0)|\mathbf{k}+\mathbf{G}|^2 \tag{6b}$$

for the H and E polarization, respectively. If all materials are isotropic, then for both E and H polarizations, we have the same dispersion relation in the absence of the spatial modulation, $\varepsilon_o\omega^2=|\mathbf{k}+\mathbf{G}|^2$, where $\varepsilon_o=1/\kappa(0)$. This relation for a symmetrical $\mathbf{k}$ vector in a square or a hexagonal lattice can be written as

$$\varepsilon_o\omega^2=|\mathbf{k}+\mathbf{G}|^2=c_{\mathbf{k}}m_{\mathbf{k}}, \tag{7}$$

where $m_{\mathbf{k}}$ is an integer and $c_{\mathbf{k}}$ is a constant.[33] The expressions for symmetrical points of a hexagonal lattice, $\mathbf{k}(k,\theta)=\Gamma(0,0)$, $K(2/3,0)$, and $M(1/\sqrt{3},90°)$ are tabulated in Table I. The integer $m_{\mathbf{k}}$ in Eq. (7) takes only specific values and allows us to label the state of a distinct ω with an integer label, $m_{\mathbf{k}}$. The degeneracy of the state, $n(m_{\mathbf{k}})$, can then be taken as the number of possible combinations of n_1 and n_2 that lead to the same $m_{\mathbf{k}}$. Using the angle, $\alpha_{\mathbf{k}}$ we can write $m_{\mathbf{k}}$ either in n_1 or n_2 alone. As such $m_{\mathbf{k}}$ decomposes into (see Ref. 34 for a general proof)

$$m_{\mathbf{k}}=q(\alpha_{\mathbf{k}},\alpha_{\mathrm{bi}})p_{\mathbf{k}}(n_j), \tag{8}$$

where $i,j=1,2$ or 2, 1, $p_{\mathbf{k}}$ is independent of $\alpha_{\mathbf{k}}$ but depends on either n_1 or n_2, and

$$q(\alpha_{\mathbf{k}},\alpha_{\mathrm{bi}})=\mathrm{cosec}^2(\alpha_{\mathbf{k}}-\alpha_{\mathrm{bi}}),\quad \alpha_{\mathbf{k}}\neq\alpha_{\mathrm{bi}}, \tag{9}$$

in which $i=1$ or 2. Equation (8) allows us to categorize a set of parallel $\mathbf{k}+\mathbf{G}$ vectors with the same $\alpha_{\mathbf{k}}$ (and hence the same q). Therefore, the expressions for distinct $m_{\mathbf{k}}$'s of the same $\alpha_{\mathbf{k}}$ will be similar with the differences only in $p_{\mathbf{k}}$, representing the relative differences in the length of the $\mathbf{k}+\mathbf{G}$ vectors. If we define $p_{\mathbf{k},s}$ and $m_{\mathbf{k},s}$ to be the smallest value among the values of $p_{\mathbf{k}}$ and $m_{\mathbf{k}}$ of the same $\alpha_{\mathbf{k}}$, then we can define a useful ratio, $p_{\alpha_{\mathbf{k}}}=\sqrt{p_{\mathbf{k}}/p_{\mathbf{k},s}}=\sqrt{m_{\mathbf{k}}/m_{\mathbf{k},s}}$ to define any vector $\mathbf{k}+\mathbf{G}$ with angle $\alpha_{\mathbf{k}}$ as $\mathbf{k}+\mathbf{G}=p_{\alpha_{\mathbf{k}}}(\mathbf{k}+\mathbf{G})_s$, where $(\mathbf{k}+\mathbf{G})_s$ is the shortest among the $\mathbf{k}+\mathbf{G}$ vectors with an angle $\alpha_{\mathbf{k}}$. On the other hand, it is worth mentioning that states with the same $\alpha_{\mathbf{k}}$ will have the same symmetry, which means the symmetry representation of these states is made of an identical composition of irreducible representations.[35]

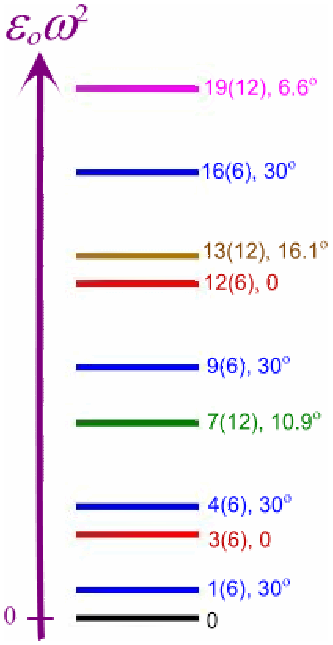

FIG. 1. (Color online) Degenerate states in the absence of the spatial modulation and material's anisotropy at the Γ point of a hexagonal lattice. The states are indexed as $m_\Gamma[n(m_\Gamma)]$, α_Γ. Each state with the same α_Γ appears with the same color. The α_Γ is calculated based on Table I with an accuracy up to 1 decimal place.

For the hexagonal lattice, the expressions for $\alpha_{\mathbf{k}}$, q, and $p_{\mathbf{k}}$ are tabulated in Table I. Figure 1 gives a visualization of the states [with indices m_{k}, $n(m_{\mathbf{k}})$, and $\alpha_{\mathbf{k}}$] using Eq. (7) in the absence of a spatial modulation for the Γ point of the hexagonal lattice. By multiplying $p_{\mathbf{k}}$ in Table I with the q, and forcing the result to be an integer, we could systematically rewrite the expressions for $m_{\mathbf{k}}$ of the same q in terms of a free integer, $h_{\mathbf{k}}$ (i.e., independent of n_1 and n_2). The result of such analysis is presented in Tables II–IV for Γ, M, and K points, respectively. Possible values of $\sin(\alpha_{\mathbf{k}})$ and $\alpha_{\mathbf{k}}$ are calculated using the expressions in Table I and due to the symmetry of both lattice and the **k** vector (i.e., point group of **k**),[35] the $\alpha_{\mathbf{k}}$ angles in Tables II–IV are restricted between $0 \le \alpha_\Gamma \le 30°$, $0 \le \alpha_K \le 60°$, and $0 \le \alpha_M \le 90°$ for Γ, K, and M points, respectively. Considering the state of $a_\Gamma = 10.9°$, the result of $m_\Gamma = p_\Gamma(n_1)q(\alpha_{b2})$ and $m_\Gamma = p_\Gamma(n_2)q(\alpha_{b1})$ yields $7n_1^2/9$ and $7n_2^2/4$, respectively. However by forcing $n_1 = 3h_\Gamma$ and $n_2 = 2h_\Gamma$, both $p_\Gamma(n_1)q(\alpha_{b2})$ and $p_\Gamma(n_2)q(\alpha_{b1})$ reduce to $7h_\Gamma^2$ (Table II).

Figures 2(a)–2(c) show examples of $\mathbf{k}+\mathbf{G}$ vectors for the states of Γ point with $\alpha_\Gamma = 30°$, 0, and 10.9°, respectively.

TABLE II. The expressions for m_Γ in terms of a free integer, h_Γ ($h_\Gamma = 1,2,3,\ldots$).

$\sin(\alpha_\Gamma)$	$1/2$	0	$1/(2\sqrt{7})$	$1/\sqrt{13}$	$1/(2\sqrt{19})$
$\alpha_\Gamma(°)$	30	0	10.9	16.1	6.6
$q(\alpha_{b1})$	4/3	4	7/3	52/27	76/27
$q(\alpha_{b2})$	4/3	1	28/27	13/12	76/75
m_Γ	h_Γ^2	$3h_\Gamma^2$	$7h_\Gamma^2$	$13h_\Gamma^2$	$19h_\Gamma^2$

The vectors connecting the origin (green marker) and the edges of each closed polygon in these figures represent the $\mathbf{k}+\mathbf{G}$ vectors. Edges of the same polygon necessarily have the same $m_{\mathbf{k}}$ (i.e., same length), and hence correspond to a single state. Within each figure, we have many isomorphic but scaled polygons, with different values of h_Γ. Though each edge of the same polygon represents a symmetrical $\mathbf{k}+\mathbf{G}$ vector with different $\alpha_{\mathbf{k}}$, due to the symmetry of **k** vector, we limit α_Γ to be $0 \le \alpha_\Gamma \le 30°$. For example, in Fig. 2(a), the angle of $\mathbf{k}+\mathbf{G}$ vectors can be 30°, 90°, 150°, 210°, 270° or 330°, but α_Γ is fixed as 30°.

IV. PRESENCE OF SPATIAL MODULATION

A. Solution at symmetrical points

The solution at the symmetrical points is crucial as band gap openings[1–3] and unusual conductions like superprism[26–28] and negative refractions[12] occur near the band edges (i.e., symmetrical points). Further, once the solution at a symmetrical **k**-point is known, then the solution for **k** vectors in the neighborhood of the symmetrical point can be easily obtained by means of other methods such as perturbation theory.[36] In this section, we introduce a simple yet powerful method to approximate the solutions at symmetrical **k**-points of a 2D PC with isotropic materials and in the subsequent sections, the nonsymmetrical **k** vectors will be handled and the influence of the material's anisotropy will be considered.

From Eq. (4), we write

$$H_i = \frac{\sum_{i \neq j} M_{ij} H_j}{\{\omega^2 - M_{ii}\}}, \tag{10}$$

where the size of matrix, M, is ideally infinite. For the 2D PC with all isotropic materials, we have

TABLE III. The expressions for m_M in terms of a free integer, h_M ($h_M = 1,2,3,\ldots$). Key: ND—not defined.

$\sin(\alpha_M)$	1	0	$2/\sqrt{7}$	$1/\sqrt{13}$	$4/\sqrt{19}$
$\alpha_M(°)$	90	0	49.1	16.1	66.6
$q(\alpha_{b1})$	4/3	4	28/27	52/27	76/75
$q(\alpha_{b2})$	ND	1	7/3	13/12	19/3
m_M	$(2h_M+1)^2$	$3(2h_M+1)^2$	$7(2h_M+1)^2$	$13(2h_M+1)^2$	$19(2h_M+1)^2$

TABLE IV. The expressions for m_K in terms of a free integer, h_K (or h'_K) ($h_K=0,1,2,3,\ldots$, $h'_K=-1,-2,-3,\ldots$).

$\sin(\alpha_K)$	0	$\sqrt{3}/2$	$(1/2)\sqrt{3/7}$	$(3/2)\sqrt{3/13}$	$\sqrt{3/19}$
$\alpha_K(^\circ)$	0	60	19.1	46.1	23.4
$q(\alpha_{b1})$	4	1	7/4	52/49	76/49
$q(\alpha_{b2})$	1	4	28/25	52/25	19/16
m_K	$(3h_K+1)^2$	$(3h'_K+1)^2$	$7(3h_K+1)^2$	$13(3h_K+1)^2$	$19(3h_K+1)^2$

$$H_i = \frac{\sum_{i\neq j} M_{ij}H_j}{\omega^2 - \kappa_0|\mathbf{k}+\mathbf{G}_i|^2} = \frac{\varepsilon_o \sum_{i\neq j} M_{ij}H_j}{\{\varepsilon_o\omega^2 - c_{\mathbf{k}}m_{\mathbf{k}}\}}. \tag{11}$$

At symmetrical **k**-points with small spatial modulation, $\varepsilon_o\omega^2 \approx c_{\mathbf{k}}m_{\mathbf{k}}$ [see Eq. (7)] and hence, only $n(m_{\mathbf{k}})$—number of H_i will be dominant [since there are $n(m_{\mathbf{k}})$ combinations of **G** leading to the same $m_{\mathbf{k}}$], and therefore Eq. (4) can be approximately written as

$$\sum_{j=1}^{n(m_{\mathbf{k}})} M_{ij}H_j = \omega^2 H_i. \tag{12}$$

Equation (12) is a secular equation that solves each state, $m_{\mathbf{k}}$ with a matrix size $n(m_{\mathbf{k}})$ by $n(m_{\mathbf{k}})$. In formulating the matrix elements of Eq. (12), the vector **G** must be chosen such that they all have the same $m_{\mathbf{k}}$ (i.e., equal length of $\mathbf{k}+\mathbf{G}$). Equation (8) enables us to generalize the form of solution for Eq. (12) with a particular $m_{\mathbf{k}}$, available for other states with the same $\alpha_{\mathbf{k}}$.

If we define a set of **G** vectors as a set of fundamental vectors that leads to the smallest $m_{\mathbf{k}}$ within the states having the same $\alpha_{\mathbf{k}}$ (i.e., $p_{\mathbf{k}}=p_{\mathbf{k},s}$ and $m_{\mathbf{k}}=m_{\mathbf{k},s}$), then the secular equation [i.e., Eq. (12)] becomes

$$\sum_{j=1}^{n(\alpha_{\mathbf{k}})} \overline{M}_{ij}^{\alpha_{\mathbf{k}}} H_j = \left(\frac{\omega_{\mathbf{k}}}{c_{\mathbf{k}}m_{\mathbf{k}}}\right)^2 H_i, \tag{13}$$

where we have assumed states with the same α_k have the same degeneracy $n(m_{\mathbf{k}})=n(\alpha_{\mathbf{k}})$, and the definition of $\overline{M}_{ij}^{\alpha_{\mathbf{k}}}$ takes the forms of

$$\overline{M}_{ij}^{\alpha_{\mathbf{k}}} = \begin{cases} \mathbf{e}_i \cdot \tilde{\kappa}_H[p_{\alpha_{\mathbf{k}}}(\mathbf{G}_i - \mathbf{G}_j)] \cdot \mathbf{e}_j, & H \text{ polarization}, \\ \kappa_E[p_{\alpha_{\mathbf{k}}}(\mathbf{G}_i - \mathbf{G}_j)], & E \text{ polarization}, \end{cases} \tag{14}$$

where the vector $\mathbf{G}_i$ with $i=1,2,\ldots,n(\alpha_{\mathbf{k}})$ denotes a set of fundamental vectors with the smallest $m_{\mathbf{k}}$ among the set of vectors with the same $\alpha_{\mathbf{k}}$. For instance, the set of fundamental vectors for a state with $\alpha_\Gamma=30°$ will be the vectors indicated by the edges of the smallest polygon in Fig. 2(a). These vectors $\mathbf{G}_1$, $\mathbf{G}_2$, $\mathbf{G}_3$, $\mathbf{G}_4$, $\mathbf{G}_5$, and $\mathbf{G}_6$ have (n_1,n_2) indices $(0,-1)$, $(1,0)$, $(1,1)$, $(0,1)$ $(-1,0)$, and $(-1,-1)$, respectively. The solution to Eq. (13) can be easily obtained and typical analytical solutions can be obtained for $n(\alpha_{\mathbf{k}})=2$, 3, 4 or 6.

For the hexagonal lattice, we have $p_{\alpha_{\mathbf{k}}}=h_\Gamma$, $2h_M+1$, and $3h_K+1$ (Tables II–IV) for Γ, *M* and *K* points, respectively, and the states with $n(\alpha_{\mathbf{k}})=2$, 3, 4, and 6 are analytically solvable. Throughout this paper, we will use the state $\alpha_\Gamma=30°$ $[m_\Gamma=h_\Gamma^2, n(\alpha_\Gamma)=6]$ as an example unless otherwise stated. In the absence of modulation, these states are indicated as blue lines in Fig. 1 and they are the most frequently occurring states in the first ten states at Γ point (see Fig. 1). The particular interest at Γ point is also due to the fact that

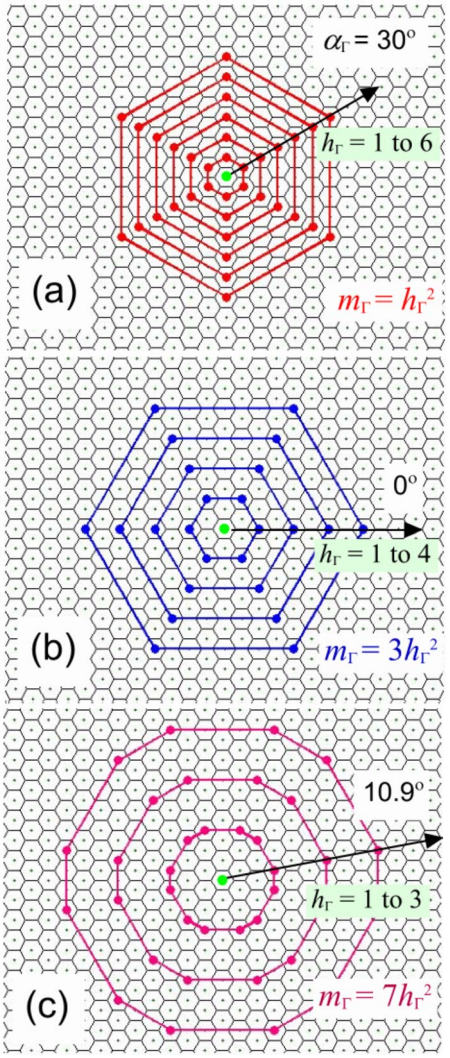

FIG. 2. (Color online) $\mathbf{k}+\mathbf{G}$ vectors for the states at the Γ point of a hexagonal lattice. The states are labeled with the angle $\alpha_{\mathbf{k}}$ [i.e., the angle made by the arrow with the k_x axis]. The green marker is taken as the origin of the reciprocal plane. (a), (b), and (c)—the states for $\alpha_\Gamma=30°$, 0, and 10.9°, respectively.

many interesting phenomena like circular equal frequency surface (i.e., the origin for negative refractive index) and cut-off conditions for diffractions at normal incidence are based on the solutions at this point. Nevertheless, similar analyses at other symmetrical **k**-points can be handled in a similar manner and in fact the systems with $n(\alpha_{\mathbf{k}})=2$, 3, and 4 (Tables II–IV) at other **k**-points have smaller matrix sizes and are therefore easier to handle.

For the state of $\alpha_\Gamma=30°$, Eqs. (13) and (14) result in two 6×6 matrices corresponding to the two different polarizations. The matrix for E polarization can be diagonalized to obtain normalized frequencies,

$$\omega_{o1}^2=\frac{4}{3}h_\Gamma^2(\kappa_0-2\kappa_1+2\kappa_2-\kappa_3)\quad(1),\qquad(15a)$$

$$\omega_{o2}^2=\frac{4}{3}h_\Gamma^2(\kappa_0+2\kappa_1+2\kappa_2+\kappa_3)\quad(1),\qquad(15b)$$

$$\omega_{o3}^2=\frac{4}{3}h_\Gamma^2(\kappa_0-\kappa_1-\kappa_2+\kappa_3)\quad(2),\qquad(15c)$$

$$\omega_{o4}^2=\frac{4}{3}h_\Gamma^2(\kappa_0+\kappa_1-\kappa_2-\kappa_3)\quad(2),\qquad(15d)$$

and similarly for H polarization,

$$\omega_{o1}^2=\frac{4}{3}h_\Gamma^2(\kappa_0+\kappa_1-\kappa_2-\kappa_3)\quad(1),\qquad(16a)$$

$$\omega_{o2}^2=\frac{4}{3}h_\Gamma^2(\kappa_0-\kappa_1-\kappa_2+\kappa_3)\quad(1),\qquad(16b)$$

$$\omega_{o3}^2=\frac{4}{3}h_\Gamma^2\left[\kappa_0-\frac{1}{2}(\kappa_1-\kappa_2)-\kappa_3\right]\quad(2),\qquad(16c)$$

$$\omega_{o4}^2=\frac{4}{3}h_\Gamma^2\left[\kappa_0+\frac{1}{2}(\kappa_1+\kappa_2)+\kappa_3\right]\quad(2),\qquad(16d)$$

with the degeneracy (indicated in the bracket) in the presence of the spatial modulation. The degeneracy in the presence of the spatial modulation is a consequence of the symmetry possessed by the PC and has to be analyzed using group theoretical tools.[1,35] In Eqs. (15a)–(15d) and (16a)–(16d), $\kappa_1=\kappa[h_\Gamma(\mathbf{G}_1-\mathbf{G}_2)]$, $\kappa_2=\kappa[h_\Gamma(\mathbf{G}_1-\mathbf{G}_3)]$, and $\kappa_3=\kappa[h_\Gamma(\mathbf{G}_1-\mathbf{G}_4)]$. In the absence of the spatial modulation, $\kappa_1=\kappa_2=\kappa_3=0$, and only κ_0 is nonzero and hence all the four solutions for E and H polarizations are equal.

In order to test the accuracy of Eqs. (15a)–(15d) and (16a)–(16d), the solutions for the state with $m_\Gamma=1$ ($\alpha_\Gamma=30°$,$h_\Gamma=1$) (Fig. 1) are analyzed for a 2D PC made of circular air holes of a filling ratio f in a matrix medium of refractive index n. Figures 3(a) and 3(b) show the result of numerical evaluation employing 361 plane waves and the result of analytical evaluation using Eqs. (15a)–(15d) and (16a)–(16d) as a function of n for the E polarization with $f=15\%$ and 23%, respectively. Figure 3(c) shows a similar plot with $f=15\%$ for H polarization. As we can readily see from these figures, Eqs. (15a)–(15d) and (16a)–(16d) provide good approximation for the values of ω_Γ for n even up to 3.0. The accuracy of the approximation reduces as the spatial modulation increases (i.e., when f or n is increased) and for a given set of the same parameters, the approximation is more accurate for E polarization than H polarization.

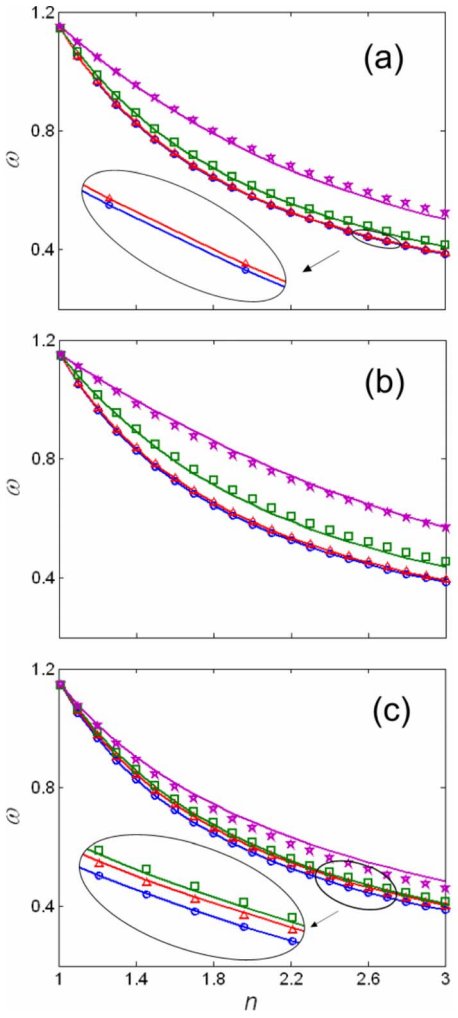

FIG. 3. (Color online) The splitting of states in the presence of the spatial modulation for the state $\alpha_\Gamma=30°$ with $h_\Gamma=1$ as a function of n. Key: solid lines—numerically evaluated using 361 plane waves; markers—analytically evaluated using Eqs. (15a)–(15d) and Eqs. (16a)–(16d). (a) E polarization with $f=0.15$, (b) E polarization with $f=0.23$. (c) H polarization with $f=0.15$.

B. Solution for k vectors in the neighborhood of symmetrical points

For **k** vectors in the neighborhood of symmetrical points, we can assume $|\mathbf{k}_n+\mathbf{k}+\mathbf{G}_i|\approx|\mathbf{k}+\mathbf{G}_i|$, where **k** and $\mathbf{k}_n$ stand for a symmetrical wave vector and a wave vector close to it (i.e., in the neighborhood region), respectively. As such, Eq. (4) can still be approximated using Eq. (13). The matrix element, $M_{ij}^{\alpha_{\mathbf{k}}}$, takes the form of

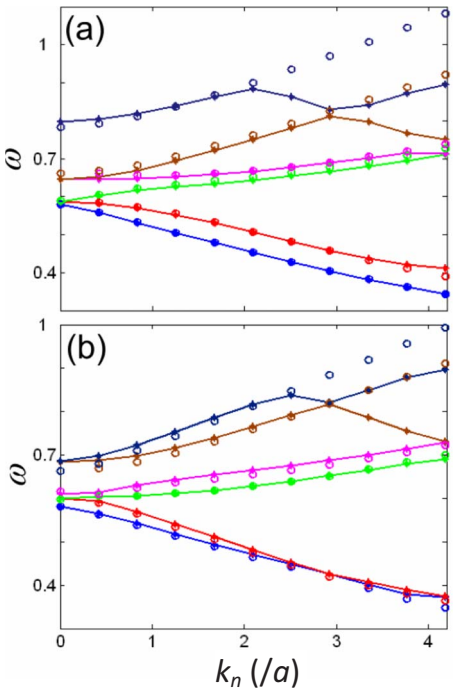

FIG. 4. (Color online) The dispersion for wave vectors in the neighborhood of Γ point for the state $\alpha_\Gamma=30°$ ($h_\Gamma=1$). The k_n vectors are along the Γ-K direction. Key: solid lines—numerically evaluated using 361 plane waves; markers—approximated using Eq. (13) with the matrix element given by Eqs. (17a) and (17b) (a) E polarization with $f=0.23$. (b) H polarization with $f=0.15$.

$$\overline{M}_{ij}^{\alpha_\mathbf{k}} = |\mathbf{k}_n + p_{\alpha_\mathbf{k}}(\mathbf{k}+\mathbf{G}_i)||\mathbf{k}_n + p_{\alpha_\mathbf{k}}(\mathbf{k}+\mathbf{G}_j)| \times\{\mathbf{e}_i \cdot \kappa[p_{\alpha_\mathbf{k}}(\mathbf{G}_i-\mathbf{G}_j)]\cdot \mathbf{e}_j\}/(c_\mathbf{k} m_\mathbf{k}), \quad (17a)$$

and

$$\overline{M}_{ij}^{\alpha_\mathbf{k}} = \kappa[p_{\alpha_\mathbf{k}}(\mathbf{G}_i-\mathbf{G}_j)]|\mathbf{k}_n + p_{\alpha_\mathbf{k}}(\mathbf{k}+\mathbf{G}_i)| \times|\mathbf{k}_n + p_{\alpha_\mathbf{k}}(\mathbf{k}+\mathbf{G}_j)|/(c_\mathbf{k} m_\mathbf{k}), \quad (17b)$$

for H and E polarizations, respectively. The size of the matrix defined by Eqs. (17a) and (17b) is $n(\alpha_\mathbf{k})$, and this significantly reduces the computational time required for diagonalizations. The result is particularly useful in calculations of an equal frequency surface, which typically involve dense $\mathbf{k}$ vectors. Equal frequency surface is commonly employed in calculating the dispersive effects of a PC such as superprism, supercolimation, etc. Interestingly, these effects occur in PCs with a small (however a finite) spatial modulation, and generally, the accuracy of the approximation provided by Eqs. (13), (17a), and (17b) will be fairly sufficient. Further, depending on $n(\alpha_\mathbf{k})$ and the $\mathbf{k}$ vector, Eqs. (17a) and (17b) can be solved exactly. The full description of the solutions for states with $n(\alpha_\mathbf{k})=2$ and the corresponding equal frequency surface have been presented by us in detail in Ref. 37.

Figures 4(a) and 4(b) show the approximated dispersion relation for E and H polarizations, respectively, for the state $m_\Gamma=1$ ($\alpha_\Gamma=30°, h_\Gamma=1$). The $\mathbf{k}_n$ was assumed to be along the Γ-K direction of the hexagonal lattice and the PC was assumed to have $n=2$ with f being 15% and 23%, the same as in Figs. 4(a) and 4(b), respectively. For a comparison, the numerically evaluated dispersion curves using 361 plane waves are also shown in these figures and we can readily see that the agreement is generally good especially for $\mathbf{k}_n$ vectors close to the Γ point.

C. Influence of anisotropy

If $\tilde{\kappa}_H$ [Eq. (5)] is taken as a sum of an isotropic tensor and an anisotropic tensor with smaller tensor components, then Eq. (12) can be used to approximate the dispersion relation in the presence of both anisotropy and spatial modulation. Though any orientation of anisotropic material can be handled by Eq. (12), in the following, we will assume a specific, yet typical orientation[28,31,38] for which the solutions can be analytically described.

Considering a 2D PC with alternating isotropic and anisotropic material in a hexagonal lattice, the coordinate system of the anisotropic material is assumed to be parallel with the coordinate system of the PC, where the principal refractive indices along the x and y axis of the PC are $n+\Delta n$ and n, respectively. As such, the matrix $\tilde{\kappa}_H$ in Eq. (5) can be written as

$$\tilde{\kappa}_H(\mathbf{G}) = \begin{pmatrix} \kappa(\mathbf{G}) + \tau(\mathbf{G}) & 0 \\ 0 & \kappa(\mathbf{G}) \end{pmatrix}, \quad (18)$$

where the matrix $\mathrm{diag}[\kappa(\mathbf{G}), \kappa(\mathbf{G})]$ is the corresponding $\tilde{\kappa}_H$ matrix for a PC with $\Delta n=0$. It is easy to see that if $\tau(\mathbf{G})$ (the coefficient representing the anisotropy) is small, then Eq. (6a) approximately equals to Eq. (7), and therefore the condition for Eq. (12) is valid. For states $m_\Gamma=h_\Gamma^2$ ($\alpha_\Gamma=30°$), being consistent with definitions of κ_0 κ_1, κ_2 and κ_3, the coefficients τ_0, τ_1, τ_2 and τ_3 can be respectively defined as $\tau_0=\tau(0)$, $\tau_1=\tau[h_\Gamma(\mathbf{G}_1-\mathbf{G}_2)]$, $\tau_2=\tau[h_\Gamma(\mathbf{G}_1-\mathbf{G}_3)]$, and $\tau_3=\tau[h_\Gamma(\mathbf{G}_1-\mathbf{G}_4)]$. In the absence of modulation, only κ_0 and τ_0 are nonzero.

With Eq. (18), Eq. (12) [or Eq. (13)] for the H polarization can be exactly solved and the solutions for states $\alpha_\Gamma=30°$ are

$$\omega_{a1} = \omega_{o1} + \frac{1}{2}(\tau_0+\tau_m^1) - \kappa_{12} + \frac{1}{6}\sqrt{32\kappa_{12}^2 + [3(\tau_0+\tau_m^1)+2\kappa_{12}]^2}, \quad (19a)$$

$$\omega_{a2} = \omega_{o2} + \frac{1}{2}(\tau_0+\tau_m^2) + \kappa_{12}' - \frac{1}{6}\sqrt{32\kappa_{12}'^2 + [3(\tau_0+\tau_m^2)-2\kappa_{12}']^2}, \quad (19b)$$

$$\omega_{a3} = \omega_{o3} + \tau_0 + \tau_m^3, \quad (19c)$$

$$\omega_{a4} = \omega_{o3} + \frac{1}{2}(\tau_0+\tau_m^1) + \kappa_{12} - \frac{1}{6}\sqrt{32\kappa_{12}^2 + [3(\tau_0+\tau_m^1)+2\kappa_{12}]^2}, \quad (19d)$$

$$\omega_{a5} = \omega_{o4} + \tau_0 + \tau_m^4, \tag{19e}$$

$$\omega_{a6} = \omega_{o4} + \frac{1}{2}(\tau_0 + \tau_m^2) - \kappa_{12}' + \frac{1}{6}\sqrt{32\kappa_{12}'^2 + [3(\tau_0 + \tau_m^2) - 2\kappa_{12}']^2}, \tag{19f}$$

with $\kappa_{12}' = \kappa_1 + \kappa_2$, $\kappa_{12} = \kappa_1 - \kappa_2$, and the modulation terms resulted from the anisotropy were summed together as τ_m^i ($i = 1, 2, 3$ or 4),

$$\tau_m^1 = \tau_1 - \tau_2 - \tau_3,$$

$$\tau_m^2 = -\tau_1 - \tau_2 + \tau_3,$$

$$\tau_m^3 = -\tau_1 + \tau_2 - \tau_3,$$

$$\tau_m^4 = \tau_1 + \tau_2 + \tau_3. \tag{20}$$

Equations (19a)–(19f) being a generalized version of Eqs. (16a)–(16d) apply for states of $\alpha_\Gamma = 30°$ with any h_Γ. The equations provide an in-depth perspective toward the understanding of the splitting of states in the presence of anisotropy and in the presence of modulation. When we switch off the material's anisotropy, Eqs. (19a)–(19f) accurately reproduce Eqs. (16a)–(16d) (H polarization) with two nondegenerate states and two doubly degenerate states. This can be seen by setting $\tau_0 = \tau_m^i = 0$, which consequently leads to $\omega_{a1} = \omega_{o1}$, $\omega_{a2} = \omega_{o2}$, $\omega_{a3} = \omega_{a4} = \omega_{o3}$, and $\omega_{a5} = \omega_{a6} = \omega_{o4}$. On the other hand, if the spatial modulation is switched off completely (i.e., $\kappa_1 = \kappa_2 = \kappa_3 = \kappa_{12}' = \kappa_{12} = \tau_m^i = 0$), then we have ω_{oi} ($i = 1, 2, 3$, and 4) $= \omega_o$ [Eqs. (16a)–(16d)] and consequently, Eqs. (19a) and (19c)–(19e) reduce to $\omega_{a1} = \omega_{a3} = \omega_{a5} = \omega_{a6} = \omega_o + \tau_o$, and Eqs. (19b) and (19f) reduce to $\omega_{a2} = \omega_{a4} = \omega_o$.

Figure 5 illustrates the results of Eqs. (19a)–(19f) and the numerical method (using 361 plane waves) for the state $h_\Gamma = 1$ ($\alpha_\Gamma = 30°$) in the hexagonal lattice PC made of circular cylinders of refractive index 2.5 in an anisotropic matrix medium of $n = 1.4$. The horizontal axis in the figure represents the variation in Δn and f. At point A, we have $f = 0.25$ and $\Delta n = 0.6$ and due to the large anisotropy, we have a deviation between the analytical approximation and the numerically evaluated curves. This deviation reduces when f (left of the point A) or Δn (right of the point A) is reduced. As we can see from the figure, when the material's anisotropy is reduced from $\Delta n = 0.6$ (at point A) to $\Delta n = 0$, the six nondegenerate states at A transform into four states composed of two nondegenerate states and two doubly degenerate states. On the other hand, when the spatial modulation is reduced from $f = 0.25$ (at point A) to $f = 0$, the six nondegenerate states transform into two states with degeneracies 4 and 2 (Fig. 5).

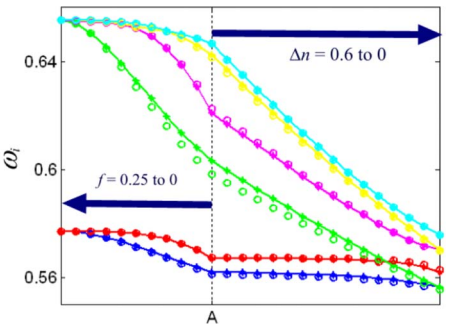

FIG. 5. (Color online) The splitting of states in the presence of modulation and in the presence of the material's anisotropy for the state $\alpha_\Gamma = 30°$ ($h_\Gamma = 1$) for H polarization and $n = 1.4$. Point A represents a configuration with $f = 0.25$ and $\Delta n = 0.6$. Key: solid lines—numerically evaluated using 361 plane waves; markers—analytically evaluated using Eqs. (19a)–(19f).

V. CONCLUSION

In summary, we have systematically analyzed the photonic states of a 2D PC. In particular, we have provided a new insight to the states, by introducing a proper classification system in the absence of a spatial modulation. States within the same class can be solved in the same manner when the modulation and the material's anisotropy are switched on.

*exwsun@ntu.edu.sg

[1] K. Sakoda, *Optical Properties of Photonic Crystals* (Spinger, New York, 2001), Chaps. 2 and 3.
[2] P. R. Villeneuve and M. Piche, Phys. Rev. B **46**, 4969 (1992).
[3] M. Plihal and A. A. Maradudin, Phys. Rev. B **44**, 8565 (1991).
[4] A. Taflove and S. C. Hagness, *Computational Electrodynamics: The Finite-Difference Time-Domain Method*, 2nd ed. (Artech House, Boston, 2000), Chap. 13.
[5] M. Qiu and S. He, J. Appl. Phys. **87**, 8268 (2000).
[6] J. B. Pendry and A. MacKinnon, Phys. Rev. Lett. **69**, 2772 (1992).
[7] J. M. Lourtioz, H. Benisty, V. Berger, and J. M. Gerard, *Photonic Crystals: Towards Nanoscale Photonic Devices* (Springer, New York, 2005), Chap. 2.1.
[8] N. A. Gippius, S. G. Tikhodeev, and T. Ishihara, Phys. Rev. B **72**, 045138 (2005).
[9] S. G. Tikhodeev, A. L. Yablonskii, E. A. Muljarov, N. A. Gippius, and Teruya Ishihara, Phys. Rev. B **66**, 045102 (2002).
[10] D. M. Whittaker and I. S. Culshaw, Phys. Rev. B **60**, 2610 (1999).
[11] A. David, H. Benisty, and C. Weisbuch, Phys. Rev. B **73**, 075107 (2006).
[12] M. Notomi, Phys. Rev. B **62**, 10696 (2000).
[13] S. Foteinopoulou and C. M. Soukoulis, Phys. Rev. B **72**, 165112 (2005).
[14] W. Jiang, R. T. Chen, and X. Lu, Phys. Rev. B **71**, 245115 (2005).
[15] F. García-Santamaría, J. F. G. López, P. V. Braun, and C. López, Phys. Rev. B **71**, 195112 (2005).
[16] G. Alagappan, X. W. Sun, M. B. Yu, and P. Shum, Phys. Rev. B

75, 113104 (2007).
[17] K. Sakoda, Phys. Rev. B **52**, 8992 (1995).
[18] A. E. Serebryannikov, T. Magath, and K. Schuenemann, Phys. Rev. E **74**, 066607 (2006).
[19] Z. Y. Li, L. L. Lin, and Z. Q. Zhang, Phys. Rev. Lett. **84**, 4341 (2000).
[20] Y. S. Zhou, X. H. Wang, B. Y. Gu, and F. H. Wang, Phys. Rev. E **72**, 017601 (2005).
[21] E. Yablonovitch, T. J. Gmitter, R. D. Meade, A. M. Rappe, K. D. Brommer, and J. D. Joannopoulos, Phys. Rev. Lett. **67**, 3380 (1991).
[22] V. Kuzmiak and A. A. Maradudin, Phys. Rev. B **57**, 15242 (1998).
[23] Y. C. Hsue, A. J. Freeman, and B. Y. Gu, Phys. Rev. B **72**, 195118 (2005).
[24] W. C. Sailor, F. M. Mueller, and P. R. Villeneuve, Phys. Rev. B **57**, 8819 (1998).
[25] R. D. Meade, A. M. Rappe, K. D. Brommer, J. D. Joannopoulos, and O. L. Alerhand, Phys. Rev. B **48**, 8434 (1993).
[26] M. S. Li, S. T. Wu, and A. Yi-. G. Fuh, Appl. Phys. Lett. **88**, 091109 (2006).
[27] J. J. Baumberg, N. M. B. Perney, M. C. Netti, M. D. C. Charlton, M. Zoorob, and G. J. Parker, Appl. Phys. Lett. **85**, 354 (2004).
[28] G. Alagappan, X. W. Sun, P. Shum, and M. B. Yu, Opt. Lett. **31**, 1109 (2006).
[29] Y. J. Liu and X. W. Sun, Appl. Phys. Lett. **89**, 171101 (2006).
[30] Z. Y. Li, J. Wang, and B. Y. Gu, Phys. Rev. B **58**, 3721 (1998).
[31] H. Takeda and K. Yoshino, Phys. Rev. E **67**, 056607 (2003).
[32] G. Alagappan, X. W. Sun, P. Shum, M. B. Yu, and D. den Engelsen, J. Opt. Soc. Am. A **23**, 2002 (2006).
[33] The labeling system with integers $m_{\mathbf{k}}$ for the states in the absence of spatial modulation in a hexagonal lattice 2D PC and the corresponding symmetry analyses were introduced previously by us. See G. Alagappan, X. W. Sun, and H. D. Sun, Phys. Rev. B **77**, 195117 (2008).
[34] Equation (8) can be derived for an arbitrary wave vector and a general 2D lattice. To see this, assuming $\mathbf{b}_1=[b_{1x},b_{1y}]$, $\mathbf{b}_2=[b_{2x},b_{2y}]$, and $\mathbf{k}=[k_x,k_y]$, consequently $\mathbf{k}+\mathbf{G}=[k_x+n_1b_{1x}+n_2b_{2x},\ k_y+n_1b_{1y}+n_2b_{2y}]$ and $\tan(\alpha_{\mathbf{k}})=k_y+n_1b_{1y}+n_2b_{2y}/(k_x+n_1b_{1x}+n_2b_{2x})$. Using $\tan(\alpha_{\mathbf{k}})$, we can write n_2 in terms of n_1 (or n_1 in terms of n_2). For example by eliminating n_2, $|\mathbf{k}+\mathbf{G}|^2=\{k_xb_{2y}-k_yb_{2z}+n_1(b_{1x}b_{2y}-b_{2x}b_{1y})\}\mathrm{cosec}^2(\alpha_{\mathbf{k}}-\alpha_{b2})/|\mathbf{b}_2|^2$.
Hence, $q(\alpha_{b2})=\mathrm{cosec}^2(\alpha_{\mathbf{k}}-\alpha_{b2})$ and $c_{\mathbf{k}}p_{\mathbf{k}}(n_1)=\frac{\{k_xb_{2y}-k_yb_{2z}+n_1(b_{1x}b_{2y}-b_{2x}b_{1y})\}}{|\mathbf{b}_2|^2}$.
[35] K. Sakoda, Phys. Rev. B **52**, 7982 (1995).
[36] L. Marchildon, *Quantum Mechanics* (Springer, New York, 2002), Chap. 10.
[37] G. Alagappan, X. W. Sun, and M. B. Yu, J. Opt. Soc. Am. A **25**, 219 (2008).
[38] C. Y. Liu and L. W. Chen, Phys. Rev. B **72**, 045133 (2005).